School of Mathematical
and Physical Sciences

Department of Mathematics and Statistics

Preprint MPS-2013-07

30 March 2013

Dependence of the climate prediction skill on spatio-temporal scales: internal versus radiatively-forced contribution

by

D. Volpi[1], F.J. Doblas-Reyes, J. Garcia-Serrano and V. Guemas

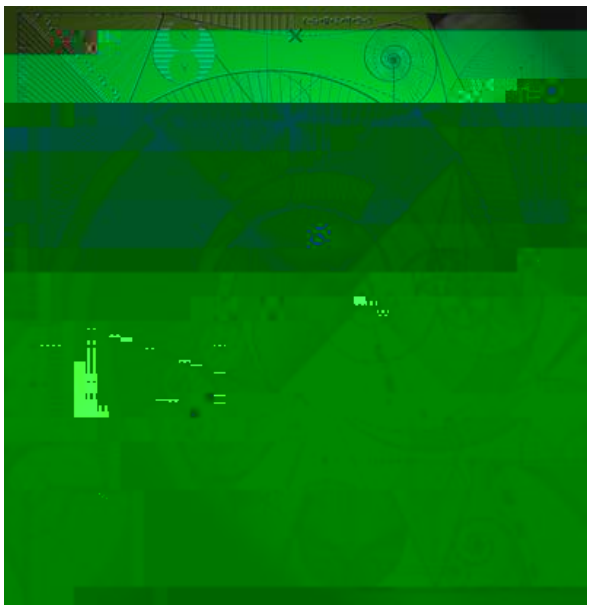

[1] PhD student at the University of Reading, working away at the Catalan Institute of Climate Sciences (IC3).

Dependence of the climate prediction skill on spatio-temporal scales: internal versus radiatively-forced contribution

D. Volpi,[1] F.J. Doblas-Reyes,[1,2]

change projections do not. The relative importance of the initial conditions in climate prediction is supposed to vary with the time scale, and has been assumed to be a continuous function that decreases with forecast time, becoming negligible after several decades [Hawkins and Sutton, 2009]. It has been shown that there is skill beyond the first forecast year and that the quality of the information about the initial state can improve the climate forecasts in di□erent regions [Doblas-Reyes et al., 2013].

This work aims at comparing the predictive skill for the near surface temperature and precipitation of an experiment initialized with observed data and one with no initialization, both experiment accounting for the variable radiative forcing. The reader has to distinguish that this is not a predictability study in the sense of Hawkins and Sutton [2009] but instead is an analysis of the actual predictive skill. The following objectives have been addressed:

- the spatial and time scales at which maximum skill is found
- a quantification of the skill improvement provided by the initialization

Section 2 presents the details of the data and the method implemented. Section 3 shows the results for near surface temperature and precipitation and section 4 aims at drawing the conclusions and suggests open issues that could lead to further work.

2. Data and method

The decadal hindcasts employed are from the perturbed-parameter ensemble of the MetO□ce Decadal Prediction System (DePreSys_

considered for the precipitation and it has been arbitrarily chosen a 3×3 grid points corresponding to approximately $1250\,\mathrm{Km} \times 1650\,\mathrm{km}$. The degrees of freedom for each spatial averaging g are then calculated as:

$$\mathrm{DOF} = \mathrm{indep}_{sd} \cdot \min\left(\frac{\mathrm{nlat} \cdot \mathrm{nlon}}{5 \cdot 5}, \mathrm{nlat}\ \cdot \mathrm{nlon}\ \right)$$

where indep_{sd} is the number of independent start dates, nlat and nlon are the number of grid points in the original grid, and nlat and nlon are the number of grid points for the degree of spatial averaging g. For precipitation this quantity is multiplied by the proportion of land data, as there is precipitation observational data available only over land.

3. Results

Fig

initialization actually corrects the sign of the NoAssim correlation. Moreover the correlation is significantly di□erent at 90% level for accumulations of up to 40 forecast months, which explains the results found for the TRO in figure 1.

The results described above are consistent across the different model version used. Figure S4 of the supplementary material shows the skill in the global domain for each individual version of the forecast system. When using the linear trend of the global-mean temperature as a proxy for the climate sensitivity, it was found that when the trend is stronger the NoAssim experiment (first column figure S4) has a larger skill at all spatial and temporal scales. Moreover, the Assim panels (second column figure S4) show that the impact of initialization is stronger when the trend is weaker. The model versions in figure S4 are ranked following the climate sensitivity estimates shown in figure S5, from the model version with higher climate sensitivity to the one with the lowest.

The NoAssim precipitation (first column figure 3) has negative correlation with the CRU data in the global domain (figure 3a) and the Tropical band (figure 3g). Some positive skill is found in the NH (figure 3d) at large-scale averaging and full forecast time accumulation. from the study as we use land only data. The correlation with CRU of the initialized experiment displays significantly positive skill (confidence level of 90%) in every domain (second column figure 3) for an accumulation of up to 20 forecast months. The maximum skill is found in the Tropics (figure 3h) for an ac-

Meehl, G., et al., 2009: Decadal prediction: can it be skillful? *Bu A r t oro o* **, 90, 1467–1485.**

Mochizuki, T., et al., 2010: Pacific decadal oscillation hindcasts relevant to near-term climate prediction. *107*, **1833–1837, doi: 10.1073/pnas.0906531107.**

Murphy, J. M., D. M. H. Sexton, D. N. Barnett, G. S. Jones, M. J. Webb, M. Collins, and D. A. Stainforth, 2004: Quantification of modelling uncertainties in a large ensemble of climate change simulations. *tur* **, 430, 768–772.**

Pohlmann, H., J. Jungclaus, A. Köhl, D. Stammer, and J. Marotzke, 2009: Initializing decadal climate predictions with the gecco oceanic synthesis: E□ects on the north atlantic. *J C* **, 22, 3926–3938.**

Robson, J. I., 2010: Understanding the performance of a decadal prediction system. Ph.D. thesis, University of Reading, dept. of Meteorology, 233 pp.

Smith, D. M., S. Cusack, A. W. Colman, C. K. Folland, G. R. Harris, and J. M. Murphy, 2007: Improved surface temperature prediction for the coming decade from a global climate model. *n* **, 317, 796–799.**

Smith, T., R. Reynolds, T. Peterson, and J. Lawrimore, 2008: Improvements to noaa's historical merged land-ocean surface temperature analysis (1880-2006). *J C* **, 21, 2283–2296.**

Taylor, K., R. Stou□er, and G. Meehl, 2012: An overview of cmip5 and the experimental design. *Bu A r t oro o* **, 93, 485–498, doi:10.1175/BAMS-D-11-00094.1.**

Teng, H. and G. Branstator, 2010: Initial-value predictability of prominent modes of north pacific subsurface temperature in a cgcm. *C D n* **, doi:10.1007/s00382-010-0749-7.**

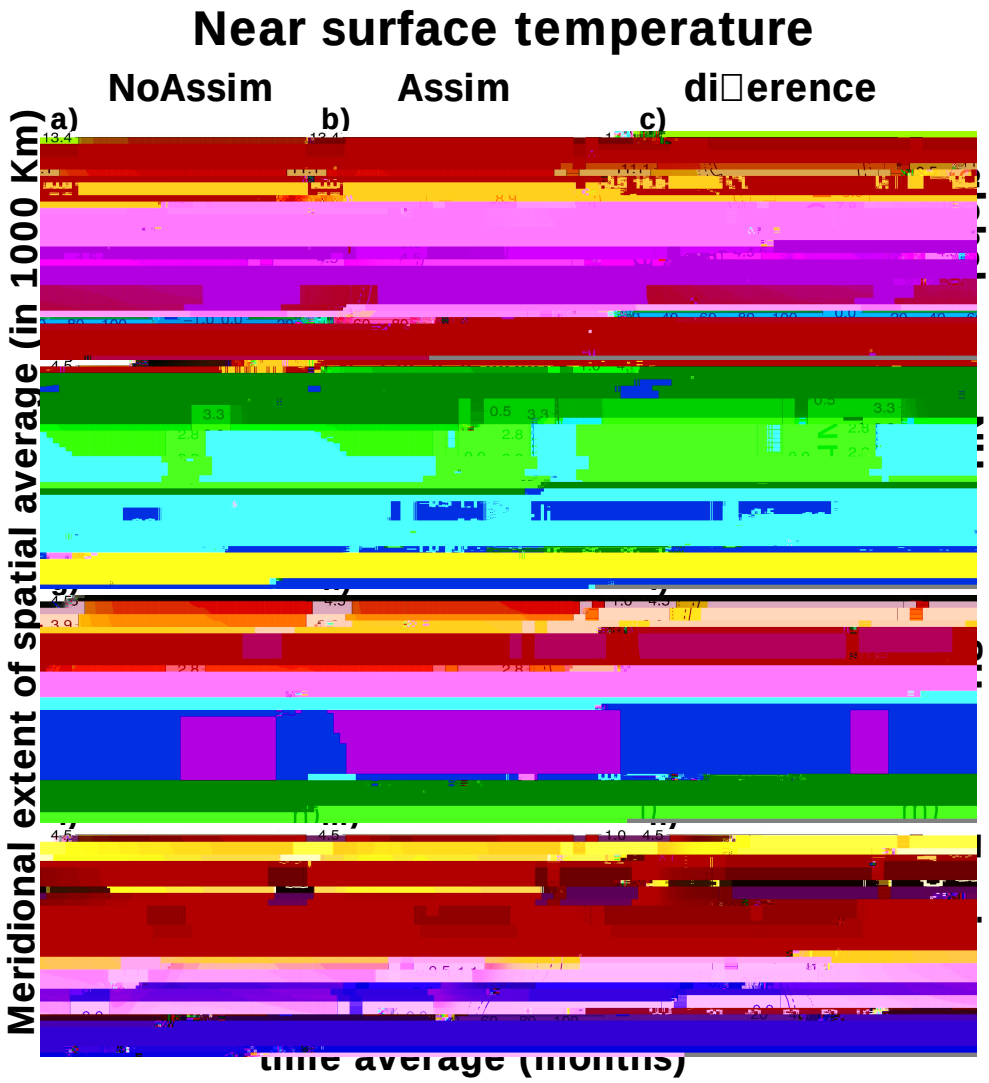

Figure 1: **Correlation of Assim and NoAssim near-surface temperature with GHCN and ERSST data depending on the forecast time and the spatial averages. a), b) c) illustrates the global domain of respectively Assim and NoAssim experiments and their di□erence. Analogously d), e), f) the Northern Hemisphere domain, g), h), i) the the Southern Hemisphere and l), m), n) the Tropical band. Note that the colour bar for the third column is di□erent from the others. The x axis indicates the number of consecutive months included in the average (from 1 up to the whole forecast period). The y axis represents the meridional extent of the spatial average at which the variances and the covariances between model and observations are computed. From those values the area average has been computed. The correlation has been calculated from the area average of the variances and covariances. The one-tailed student t-test has been computed and the black dotted, dashed and solid contours are respectively the p-value 0.01, 0.05 and 0.1. Details on the computation of the number of degrees of freedom in the text.**

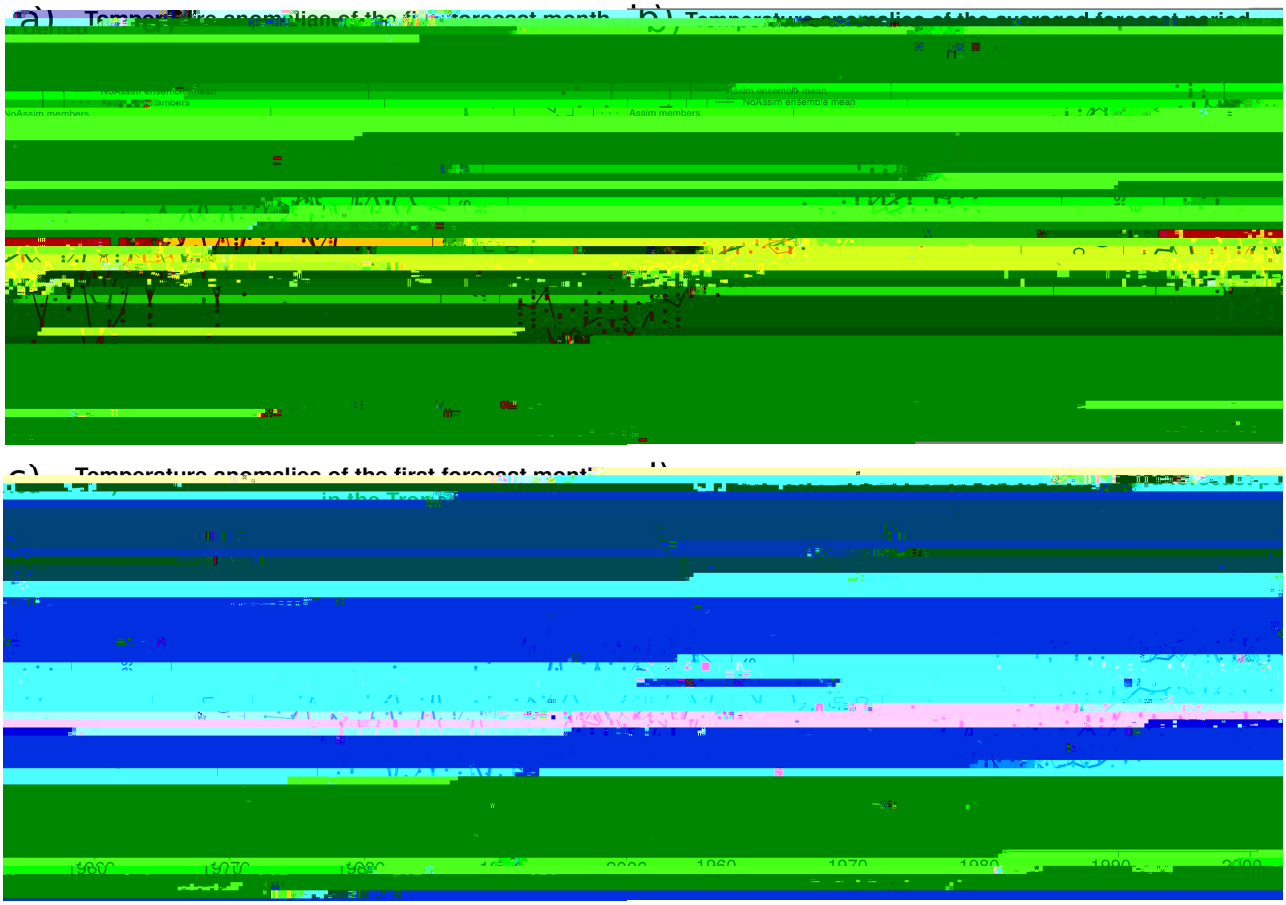

Figure 2: **Anomaly time series of Assim and NoAssim near-surface temperature with GHCN and ERSST in the global domain (a,b) and tropical band (c,d). Fgure 2a shows the time series of the first forecast month with a spatial average over the whole global domain, 2b is the anomalies timeseries of all the forecast-months average over the whole global domain. In solid black the reference data. Assim ensemble mean anomalies are is solid red while the Assim ensemble members in dotted red. Analogously the NoAssim ensemble mean anomalies are in solid blue and the NoAssim ensemble members in dotted blue. Figure 2c and 2d are the same as figure 2a and 2b but in tropical band. The year in the abscissa corresponds to the start date of each individual hindcast. Note that the legend indicates the correlation of Assim with the reference data and the correlation of NoAssim with the reference data. In panels 2a and 2c the correlation between the observed Niño3.4 SST index with the tropically averaged reference data is also shown.**